High-performance histidine-functionalized MWCNTS-GONRs/Co-Ni LDH flower cluster structural composite via microwave synthesis for supercapacitor

Hengrui Qiu, Xuejiao Sun, Shengli An, Dawei Lan, Jinlong Cui, Yongqiang Zhang[**], Wenxiu He[*]

School of Chemistry and Chemical Engineering, Inner Mongolia University of Science & Technology, Baotou, Inner Mongolia 014010, China

E-mail: wenxiu_he@foxmail.com

Fax: +86-0472-5953323

Tel: +86-0472-5953323

[*] Corresponding author at: E-mail address: wenxiu_he@foxmail.com. Tel: +86-0472-5953323. Fax: +86-0472-5953323.
[**] Corresponding author at: E-mail address: yongqiang_zhang1203@foxmail.com. Tel: +86-0472-5951506. Fax: +86-0472-5951506.

The obvious peak at about 3434 cm^{-1} is attributed to the presence of hydroxyl groups. The bands at 1720 and 1391 cm^{-1} are characteristics of the carboxy groups and O-H deformation vibration [1]. The typical C=C conjugation and C-C band are nearly 1639 and 1080 cm^{-1}, respectively [2]. In addition, the band at 1550 cm^{-1} can originate from histidine and corresponds to the C-N stretching vibration [3].

The N1s spectrum can be fitted into three peaks at 398.5, 400.1, and 401.6 eV, assigned to pyridinic, pyrrolic and graphitic N, respectively. This result demonstrates that the histidine functionalization of MWCNTs-GONRs is successful.

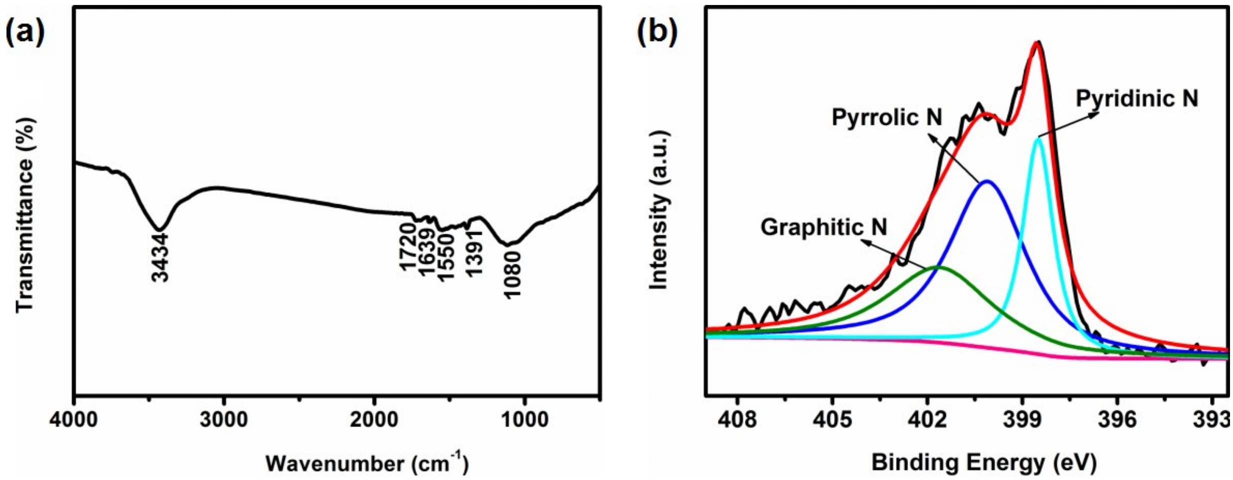

Fig. S1. The FT-IR and XPS spectra of His-MW.

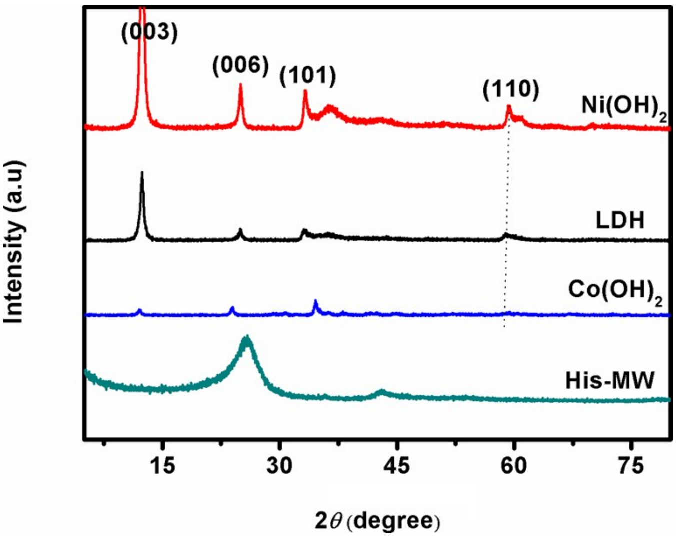

Fig. S2. XRD patterns of other materials.

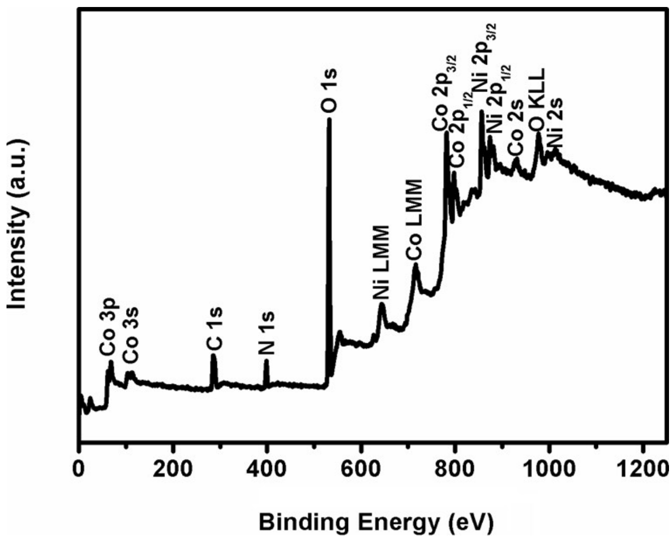

Fig. S3. survey scan of His-MW/LDH.

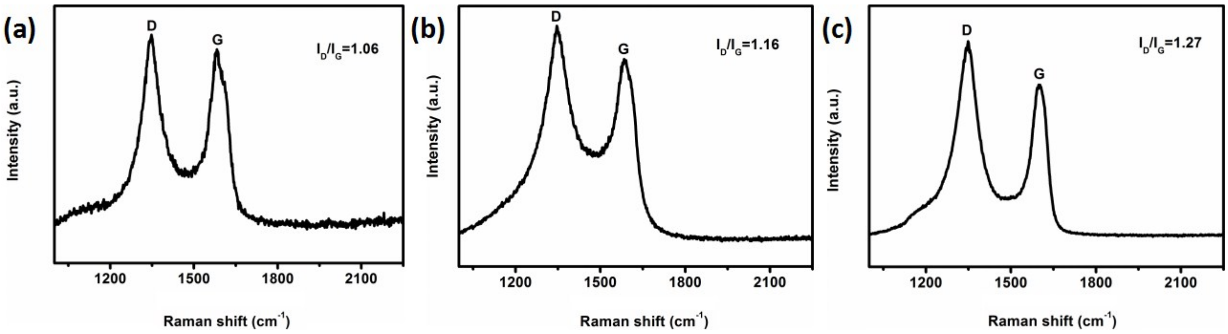

Fig. S4. Raman spectra of (a) MWCNTs-GONRs (b) His-MW and (c) His-MW/LDH.

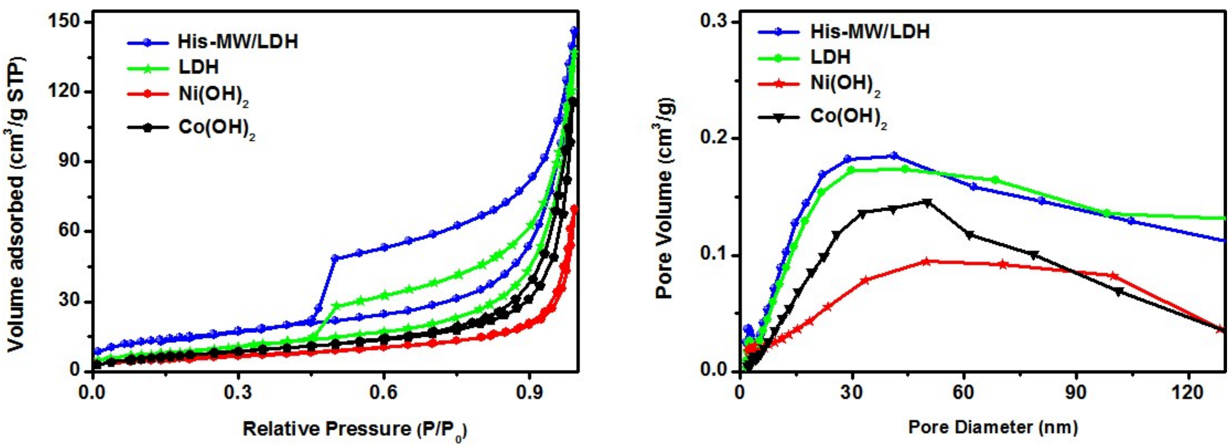

Fig. S5. (a) BET and (b) BJH curves of samples.

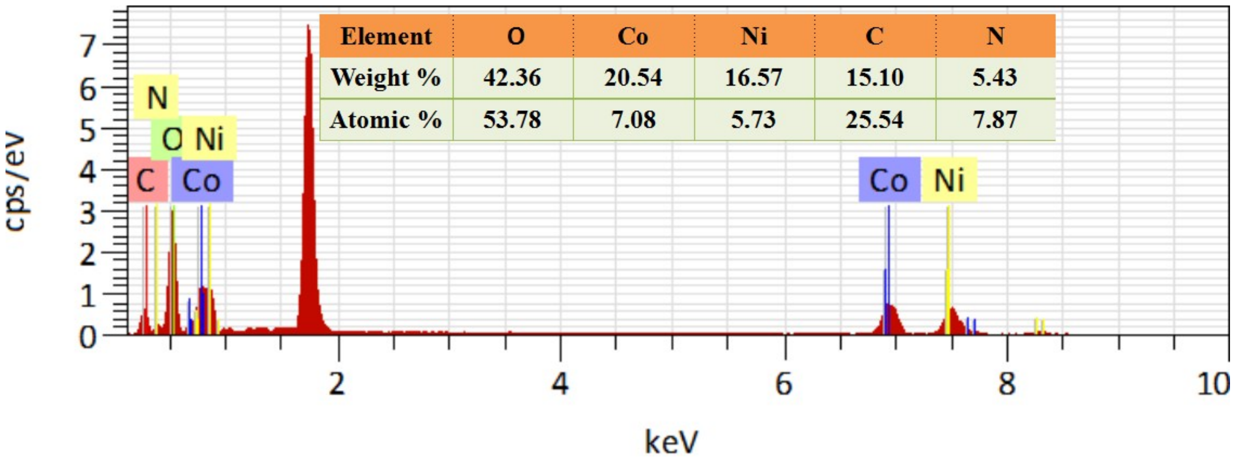

Element	O	Co	Ni	C	N
Weight %	42.36	20.54	16.57	15.10	5.43
Atomic %	53.78	7.08	5.73	25.54	7.87

Fig. S6. EDS spectrum and element concentration of His-MW/LDH.

The CV curve of nickel foam is close to a straight line, which indicates that it has a small capacitance. And the GCD curve proves the result. The EIS curve indicates its rationality as a collector fluid. Through the analysis of its electrochemical properties, we can come to a conclusion that nickel foam as a substrate will not affect the electrochemical properties of the active material.

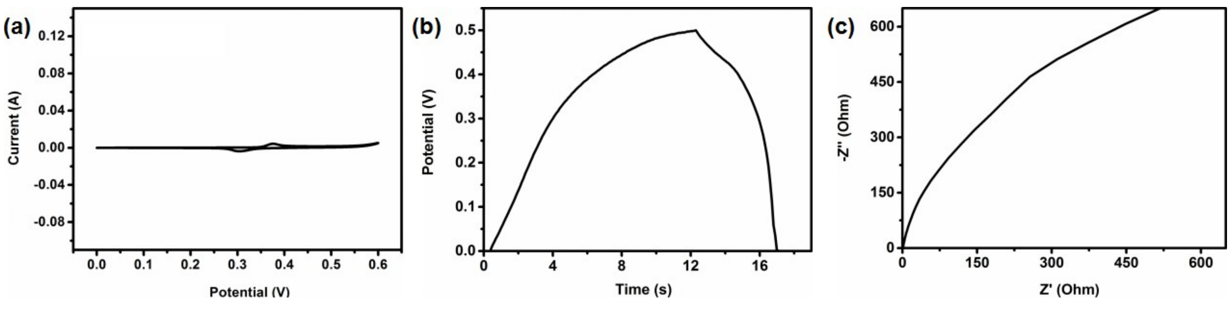

Fig. S7. The CV, GCD and EIS curves of Nickel foam.

$$i = av^b \quad (1)$$

$$\log i = b\log v + \log a \quad (2)$$

$$i(V)/v^{1/2} = k_1 v^{1/2} + k_2 \quad (3)$$

where i, v, a, b indicate the current, scanning rate, and the adjustable parameters, respectively. To obtain the value of b, the logarithm of both sides of equation (1) is taken, and subsequently linear fitting of log i and log v is done. Meanwhile, the value of b also indicates that the electrodes possess battery or pseudo-capacitor properties. The V, k_1, k_2 present the specified voltage and the adjustable parameters, respectively. In the same way, the value of k_1 can be obtained by linear fitting i(V)/$v^{1/2}$ and $v^{1/2}$ in formula (3) under the specified voltage. Finally, $k_1 v$ is the contribution of pseudocapacitor to the current at each specific voltage.

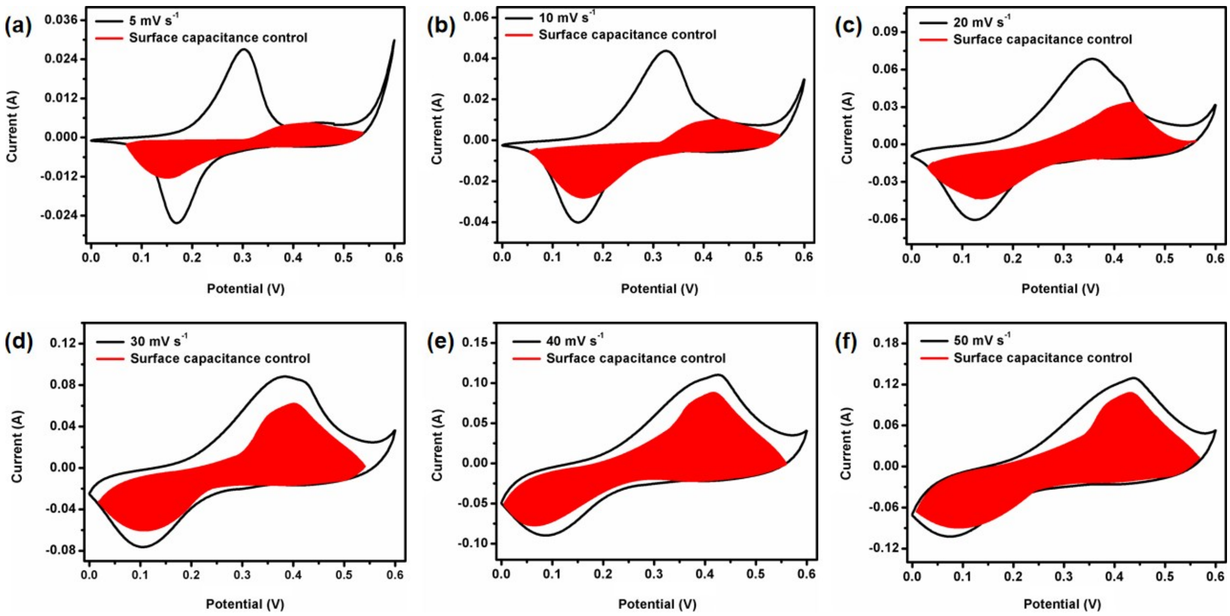

Fig. S8. The capacitance contribution to charge storage of His-MW/LDH at different scan rates.

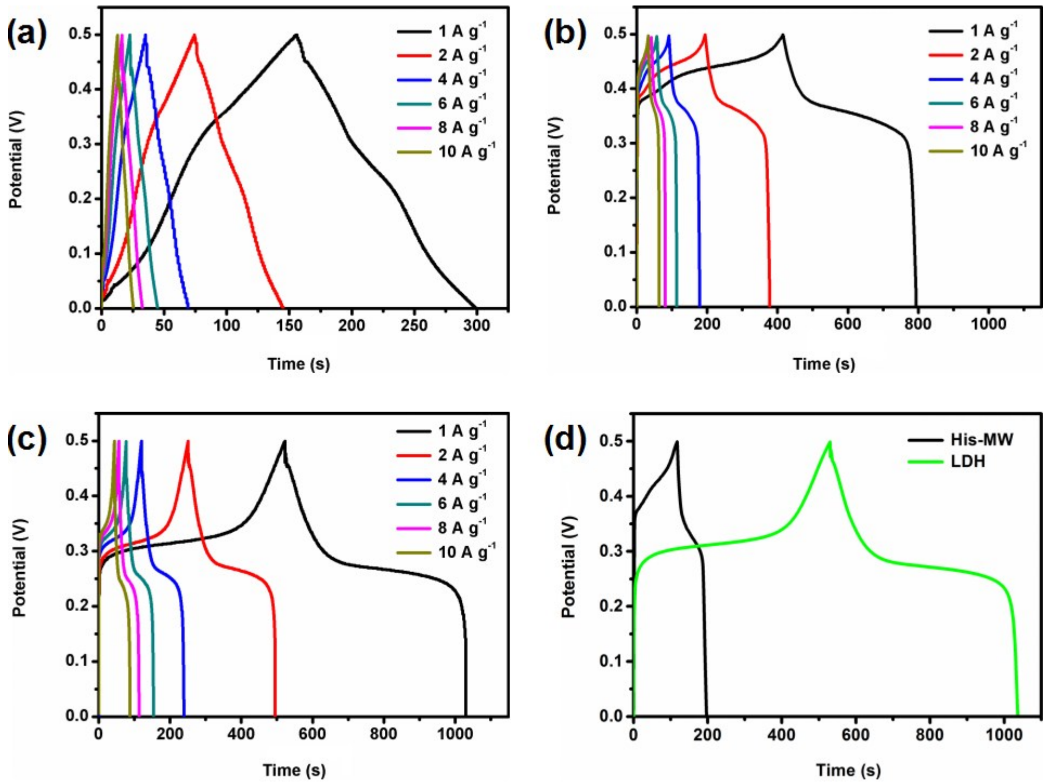

Fig. S9. The GCD curves of (a) $Co(OH)_2$, (b) $Ni(OH)_2$, (c) LDH electrodes at various current densities and (d) His-MW with LDH electrode at 1 A g^{-1}.

The curve shape and integral area of MW/LDH are similar to that of His-MW/LDH, indicating that their specific capacitance is also similar. As shown in Fig. S10b, His-MW/LDH and MW/LDH electrode possess 1674 and 1577 F g^{-1} at 1 A g^{-1}, respectively. The result show that the histidine functionalization of carbon materials plays a positive role in the electrochemical properties of the composites.

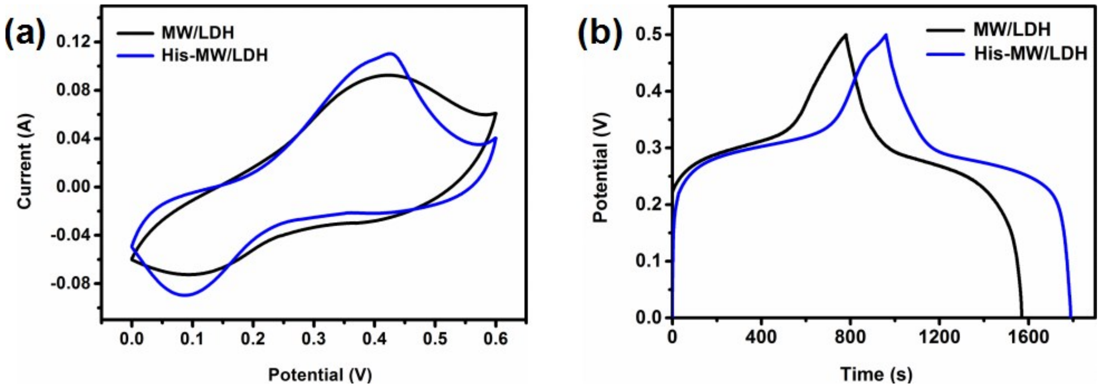

Fig. S10. The (a) CV and (b) GCD curves of MW/LDH with His-MW/LDH electrodes.

The Rs and Rct of His-MW/LDH, LDH, $Ni(OH)_2$ and $Co(OH)_2$ electrodes are 0.28, 0.61, 0.75, 0.40 Ω and 0.59, 0.93, 0.21, 0.28 Ω.

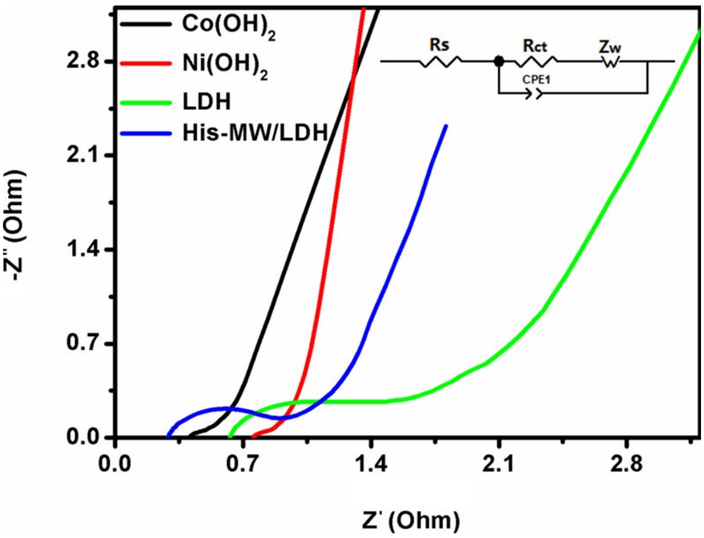

Fig. S11. Nyquist plots of electrodes.

The Rs are 0.36, 0.79, 0.95, and 0.54 Ω for the His-MW/LDH, LDH, $Ni(OH)_2$ and $Co(OH)_2$ electrodes. The Rct are 0.76, 2.23, 0.51, and 0.41 Ω for the His-MW/LDH, LDH, $Ni(OH)_2$ and $Co(OH)_2$ electrodes.

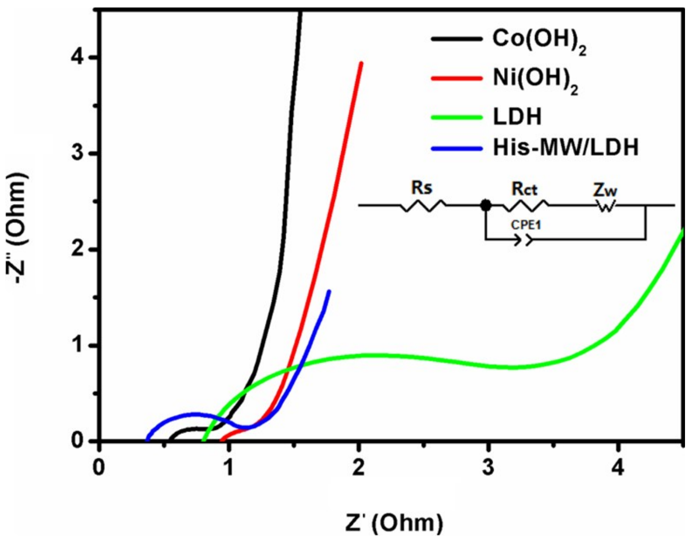

Fig. S12. The Nyquist plots of the electrodes after 2000 times cycle.

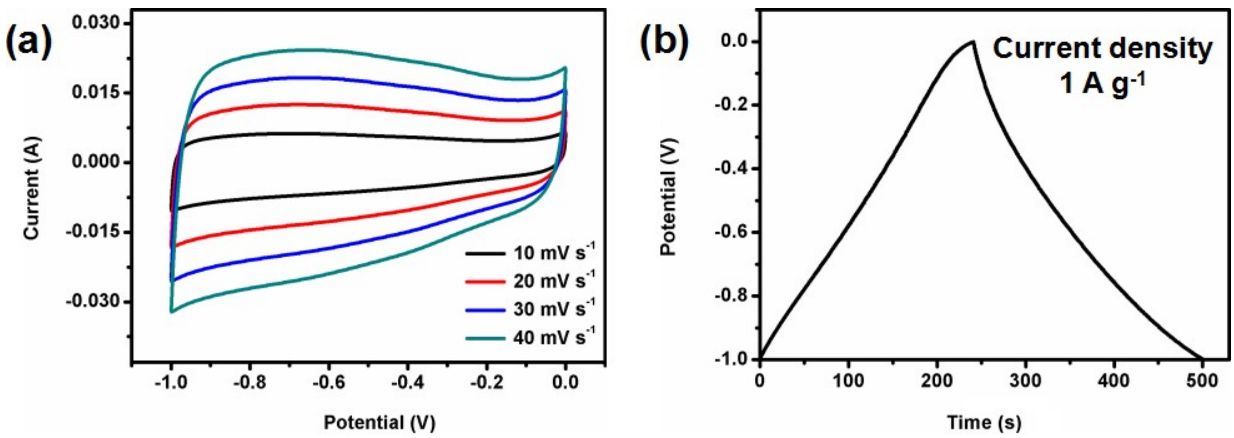

Fig. S13. CV and GCD curves of AC electrode.

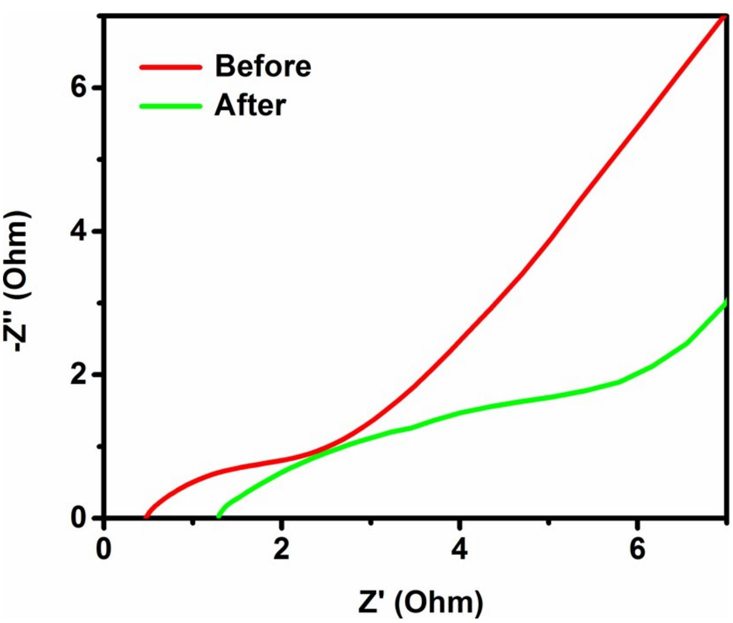

Fig. S14. EIS curves of device

Table S1

electrode	Electrolyte	Specific capacitance ($F g^{-1}$) at 1 $A g^{-1}$	Retention (%) cycling Number current density	Refs.
KCu_7S_4@NiCo-LDH	6 M KOH	1104.5	83.5% after 1000 times at 8 $A g^{-1}$	[4]
PCF@RGO/NiCo-LDH	1 M KOH	1220.5	84.1% after 5000 times at 8 $A g^{-1}$	[5]
α-Co/$Ni(OH)_2$@Co_3O_4-70	6 M KOH	1000	72.34% after 8000 times at 2 $A g^{-1}$	[6]
$Co(CO_3)_{0.5}(OH)$/$Ni_2(CO_3)(OH)_2$	6 M KOH	987	82.9% after 2000 times at 10 $A g^{-1}$	[7]
MnO_2-2/NiCo-LDH/CC	1 M KOH	217	97% after 5000 times at 2 $A g^{-1}$	[8]
ZnCo-PBA@α-$Co(OH)_2$	1 M KOH	423.92	78.48% after 1000 times at 5 $A g^{-1}$	[9]
$LaCO_3OH$-$Ni(OH)_2$@RGO	1 M KOH	572.47	80% after 2000 times at 10 $A g^{-1}$	[10]
His-MW/LDH	6 M KOH	1674	83.33% after 2000 times at 10 $A g^{-1}$	This work

Table S2

Supercapacitors	Electrolyte	Potential window (V)	Specific capacitance ($F\ g^{-1}$) at 1 $A\ g^{-1}$	Maximum energy density ($Wh\ kg^{-1}$)	Power density ($kW\ kg^{-1}$)	Retention (%) cycling Number current density	Refs.
RGO@NiMn-LDH@NF//AC	6 M KOH	1.4	84	22.5	0.7	91% after 1000 times at 1 $A\ g^{-1}$	[11]
Ni-Co LDH@rGO//rGO	poly(vinyl alcohol)/ KOH gel	1.5	112	35	0.750	80.2% after 4000 times at 5 $A\ g^{-1}$	[12]
α-Co/Ni(OH)$_2$@Co$_3$O$_4$-70//AC	6 M KOH	1.6	61.33	23.88	0.075	63% after 10000 times at 1 $A\ g^{-1}$	[6]
Co(CO$_3$)$_{0.5}$(OH)/Ni$_2$(CO$_3$)(OH)$_2$ //AC	PVA/KOH gel	1.6	110.3	39.2	0.8	83.3% after 5000 times at 10 $A\ g^{-1}$	[7]
Ni$_{0.35}$Co$_{0.65}$-LDHs//ACDC (activated cotton-derived carbon)	2 M KOH	1.6	157.5	30.63	4.9	78.62% after 5000 times at 7 $A\ g^{-1}$	[13]
Co$_3$O$_4$@glucose-modified NiMn-LDH //AC	6 M KOH	1.6	108	38.4	0.8	89.1% after 2000 times at 5 $A\ g^{-1}$	[14]
His-MW/LDH //AC	6 M KOH	1.6	111	39.47	0.8	93.81% after 6000 times at 10 $A\ g^{-1}$	This work

References

[1] D.Sajjad, Y.M. Oskoei, M. Fouladgar, J. Exp. Nanosci., 2016, 11, 1384-1401.

[2] D.B. Shinde, J. Debgupta, A. Kushwaha, M. Aslam, V.K. Pillai, J. Am. Chem. Soc., 2011, 133, 4168-4171.

[3] S. Sasha, R.D. Piner, S.T. Nguyen, R.S. Ruoff, Carbon, 2006, 44, 3342-3347.

[4] P. Yang, C. Jing, J.C. Liu, K. Chen, Y.X. Zhang, Crystengcomm, 2020, Doi:10.1039/c9ce01261c.

[5] J.Q. Qi , Y.W. Chen, Q. Li , Y.W. Sui, Y.Z. He, Q.K. Meng, F.X. Wei , Y.J. Ren, J.L. Liu, J. Power Sources, 2020, 445, 227342.

[6] Y.X. Bao, Y. Deng, M.Z. Wang, Z.Y. Xiao, M.H. Wang, Y.L. Fu, Z.Y. Guo, Y. Yang, L. Wang, Appl. Surf. Sci., 2020, 504, 144395.

[7] G.F. Zhang, P. Qin, R. Nasser, S.K. Li, P. Chen, J.M. Song, Chem. Eng. J., 2020, 124029.

[8] L.L. Liu, L. Fang, F. Wu, J. Hu, S.F. Zhang, H.J. Luo, B.S. Hu, M. Zhou, J. Alloy. Compd., 2020, 153929.

[9] X.Y. Sun, S.Q. Li, R.M. Liu, X.L. Sun, X.J. Liu, A.R. Li, W. Li, J. Nanopart. Res., 2020, 22, 37.

[10] T. Lv, Z.N. Xu, W. Hong, G.F. Li, Y.W. Li, L.S. Jia, Chem. Eng. J., 2020, 382, 123021.

[11] L. Sun, Y.X. Zhang, Y. Zhang, H.C. Si, W.P. Qin, Y.H. Zhang, Chem. Commun., 2018, 54, 10172-10175.

[12] S.K. Kiran, S. Shukla, A. Struck, S. Saxena, ACS Appl. Mater. Inter., 2019, 11, 20232-20240.

[13] Y.Y. Feng, Y.J. Li, W. Yang, H.B. Huang, J. Nanosci. Nanotechno., 2020, 20, 1260-1268.

[14] W. Quan, Y.Y. Xu, Y.T. Wang, S.C. Meng, D.L. Jiang, M. Chen, Appl. Surf. Sci., 2019,

488, 639-647.